scientific reports

Check for updates

OPEN

Parametric optimization of graphite powder-mixed electrical discharge machining of Ni-Cr dental alloy by response surface methodology

Emin Salih San[1], Hacı Bekir Özerkan[1]✉, Mehmet Subaşı[2], Emre Ayhan[3], Ahmet Mavi[4], Sachin Salunkhe[5,6]✉, Emad S. Abouel Nasr[7] & Robert Čep[8]

In this study, the effects of machining parameters on material removal rate (MRR), electrode wear rate (EWR) and surface roughness (R_a) in the electrical discharge machining (EDM) of nickel-chromium-based alloy were investigated. Discharge current (*I*), pulse-on time (T_{on}), pulse-off time (T_{off}) and graphite powder concentration were selected as variable parameters in the study. An experimental setup was designed and manufactured for use in powder-mixed EDM experiments. Mathematical models were generated using response surface methodology (RSM), the most effective parameters on the results were determined and regression equations were obtained. Parameter optimization was performed with the highest MRR, lowest EWR, and lowest R_a performance targets. The ideal machining conditions were determined as *I* = 12.5 A, T_{on}=66µs, T_{off}=6µs and powder-mixed dielectric. Using the powder-mixed dielectric, 34.54% higher MRR, 20.01% lower EWR and 12.64% lower R_a were achieved on average. Using the created mathematical model, the result of the machining to be done with these parameters was predicted and the reliability of the model was tested by comparing the predicted results of the model and the results of the verification experiment.

Keywords Electrical discharge machining, Material removal rate, Electrode wear rate, Surface roughness, Optimization, Powder-mixed ED, M (PMEDM)

Abbreviations

ANOVA	Analysis of variance
EWR	Electrode wear rate
I	Discharge current
MRR	Material removal rate
R_a	Average surface roughness
T_{on}	Pulse-on time
T_{off}	Pulse-off time
RSM	Response surface methodology

The effects of powder-mixed (PM) dielectrics on electrical discharge machining (EDM) have been studied by many researchers. Jeswani reported that the addition of graphite powder to dielectric fluid increased MRR by 60%, EWR by 15%, and decreased the MRR/EWR ratio by 28% in machining with a steel workpiece and copper

[1]Mechanical Engineering Department, Gazi University, Ankara, Turkey. [2]Department of Machine and Metal, Gazi University, Ankara, Turkey. [3]Department of Electronic and Automation, Gazi University, Ankara, Turkey. [4]Faculty of Technology, Department of Manufacturing Engineering, Gazi University, Ankara, Turkey. [5]Department of Biosciences, Saveetha School of Engineering, Saveetha Institute of Medical and Technical Sciences, Chennai, India. [6]Department of Mechanical Engineering, Gazi University Faculty of Engineering, Ankara, Maltepe, Turkey. [7]Department of Industrial Engineering, College of Engineering, King Saud University, P.O. Box 800, Ri- yadh 11421, Saudi Arabia. [8]Department of Machining, Assembly and Engineering Metrology, Faculty of Mechanical Engineering, VSB-Technical University of Ostrava, 17. Listopadu 2172/15, Ostrava 708 00, Czech Republic. ✉email: ozerkan@gazi.edu.tr; sachinsalunkhe@gazi.edu.tr

electrode[1]. Kansal et al. showed that when silicon powder-mixed dielectric was used in the machining of EN-31 tool steel workpiece, improvement in MRR and R_a was achieved. powder concentration and I were the most effective parameters according to ANOVA results[2]. Kung et al. reported that the effect of aluminium powder addition on the MRR and EWR in machining of tungsten carbide workpiece increased as particle size, *I* and T_{on} increased; MRR increased up to a powder concentration of 15 g/l and then decreased, while the EWR decreased up to a powder concentration of 15 g/l and then increased[3]. Kumar and Davim emphasized that the use of silicon powder additive in EDM machining of Al-SiC composite increased the MRR by three times and reduced R_a by one-third, and that the most effective variables in this process were powder concentration and current[4]. Bhattacharya et al. performed machining on mould steels with different electrodes (copper, copper-tungsten) and powder additives (graphite, aluminium). The highest MRR was obtained with aluminium powder. They emphasized that the graphite powder additive reduced MRR and R_a, and that the effect of the electrode material on the outputs was weak[5]. Singh and Yeh modelled the machining of aluminium matrix composites using the GRA method. They reported that the most effective machining parameters were T_{on}, electrode retraction time, and powder size. Coarser powders decreased MRR and increased R_a. When machining was done with ideal parameters, MRR increased from 0.4267 to 0.530 g/min, EWR decreased from 0.0112 to 0.0096 g/min, and Ra decreased from 3.64 to 2.82 µm[6]. Assarzadeh and Ghoreishi modelled the machining of CK45 steel using RSM, finding that *I* and T_{on} were the most influential parameters on MRR, while *I* was the most influential on R_a. Increasing the voltage decreased MRR. The researchers calculated the maximum error rate of the developed model as 10.71% for MRR and 8.41% for R_a[7]. Jabbaripour et al. compared the effect of different powder additives (aluminium, graphite, SiC, chromium, and iron) on the machining of titanium aluminide material and stated that aluminium powder provided the highest MRR and the lowest R_a[8]. Singh et al. reported that the use of graphite powder -mixed dielectric in the machining of Superco 605 alloy reduced R_a, and that R_a increased as *I* increased. The researchers determined the ideal machining parameters to be $I = 9$ A and T_{on}=20µs, as identified through Taguchi analysis, which improved R_a from 2.23 to 1.99 µm[9]. Talla et al. modelled the EDM of aluminium-alumina composite using the GRA method, calculated the ideal machining parameters as $I = 3$ A and T_{on}=150µs, and reported that aluminium powder additive provided positive effects on both MRR and R_a[10]. Ünses and Çoğun stated that graphite powder addition increased MRR and decreased R_a in the machining of Ti-6Al-4 V alloy, but EWR also increased[11]. Long et al. achieved a 32.1% improvement in MRR when using 10 g/l titanium powder additive in EDM of various die steels[12]. S. Tripathy and D. K. Tripathy determined the ideal machining parameters for the chromium powder-mixed EDM of H-11 die steel as C_p=6 g/l, $I = 6$ A, T_{on}=100µs by the GRA method and C_p=6 g/l, $I = 3$ A, T_{on}=150µs by the TOPSIS method. Desirability of the outputs improved by 16.17% and 25.93%, respectively[13]. Mohal and Kumar stated that carbon nanotube addition increased MRR and decreased R_a in the EDM of Al-SiC material. As a result of RSM analysis, 38.22% improvement in MRR and 46.04% improvement in R_a were achieved. *I* was determined to be the most effective parameter on machining[14]. Banh et al. reported that increasing the titanium powder additive from 2 g/l to 6 g/l in the machining of die steels increased the MRR by 68%, reduced the EWR by 28% and improved the R_a[15]. Mohanty et al. modelled the EDM of Al-SiC material with RSM and showed that the powder additive had a positive effect on MRR and R_a by increasing the spark gap[16]. Jadam et al. reported that 0.5 g/l carbon nanotube addition increased MRR by 44.95%, decreased EWR by 64.1% and Ra by 14.1% in the machining of Inconel 718 alloy[17]. Sahu and Datta reported that graphite addition increased MRR by 13.08%, decreased EWR by 92.68% and R_a by 49.15% in the EDM machining of Inconel 718 alloy, and all three outputs increased with increasing *I*[18]. Alhodaib et al. performed GRA analysis on the silicon powder-mixed EDM of Nimonic-90 alloy, calculated the ideal machining parameters as C_p=12 g/l, $I = 3$ A, T_{on}=35µs and T_{off}=49µs, and achieved 50.04% improvement in R_a[19]. Ramesh and Jenarthanan modelled the machining of Nimonic alloy with various powder mixtures (graphite, silicon, manganese) using RSM and determined the ideal machining parameters as 3 g/l manganese powder, $I = 3$ A, 90% duty cycle. They determined the error rate of the generated model to be at most 6% and stated that the highest MRR was obtained with silicon and the lowest R_a was obtained with graphite powder[20]. Chakraborty et al. compared efficiency of two different methods, namely RSM and GRA-PCA for modelling WEDM of Ti6Al4V alloy. Optimum machining parameters were found as T_{on}=30µs, T_{off}=11µs, $I = 1$ A, C_p=2 g/l by RSM and outputs were 1.384 µm surface roughness and 8042 µm^2 corner inaccuracy. Optimum machining parameters found by GRA-PCA were T_{on}=30µs, T_{off}=2µs, $I = 3$ A, C_p=4 g/l and outputs were 1.315 µm surface roughness and 11,623 µm^2 corner inaccuracy. They reported that GRA-PCA method was better for modelling this process due to having a lower error rate of 3.94%, compared to 4.78% error rate of RSM model, and achieving lower R_a[21]. In further studies, Chakraborty et al. used Teaching and Learning Based Optimization technique in addition to RSM to model WEDM of Ti6Al4V. They found optimum machining parameters to be T_{on}=30.23µs, T_{off}=3.02µs, V = 79.9 V, C_p=3.1 g/l and outputs were found as 1.199 µm surface roughness and 12982.67 µm^2 corner inaccuracy. They stated that usage of powder additive improved surface quality by 50.77% and corner accuracy by 23.01%[22]. Le et al. investigated the machinability of SKD61 steel in tungsten carbine powder mixed EDM. Researchers selected *I*, T_{on} and C_p as variable parameters and used reverse polarity copper electrodes. They determined optimal inputs as $I = 1$ A, T_{on}=30µs, C_p=13.6 g/l by DA, $I = 1$ A, T_{on}=20µs, C_p=20/l by TOPSIS and $I = 1$ A. It was stated that DA provided better EWR (0.000119419 g/min and 41.5% reduction) and better MRR (0.0013641 g/min and 22.7% increase) while TOPSIS provided better R_a (0.9326 µm and 13.89% reduction) and better surface quality (lesser number of crack and thinner recast layer). It was also emphasized that *I* had the highest effect on all three output parameters while C_p contributed least to MRR while T_{on} contributed the least to EWR and R_a[23]. In another study by Le et al., effects of machining parameters (*I*, T_{on}, C_p, electrode material) on MRR, EWR and surface features were investigated in PMEDM of X40CrMoV51 steel. It was reported that 121.35% higher MRR and 46.08 lower EWR was achieved with graphite electrode, however copper electrode provided 12.52% lower recast layer thickness and a better surface uniformity[24]. This study aimed to determine the optimum machining parameters for EDM of a nickel-based dental alloy, to achieve high MRR, low EWR and low R_a and to determine the effects of graphite powder additives

on machining. The study used the "remanium® CSE" alloy, which had not previously been machined using EDM. It was aimed to show that EDM can be used as an alternative method in the high precision machining of this alloy. EDM is one of the most common unconventional manufacturing methods, allowing for the machining of materials with high surface hardness. Its advantages, such as the absence of mechanical contact and its suitability for machining complex 3D geometries, make it widely used in the mould-making, automotive and aerospace industries[25]. In this study, both graphite powder-mixed and non-powder mixed EDM experiments were conducted using copper electrodes. A special experimental setup consisting of a dielectric tank, a circulation pump, and a sprayer was designed and used for the powder-mixed EDM experiments. Graphite powder concentration, I, T_{on}, and T_{off} were set as variable parameters in the experiments, while open circuit and discharge voltages were kept constant. MRR, EWR, and R_a were measured. The findings and the effects of the parameters were evaluated using analysis of variance (ANOVA). Furthermore, a mathematical model was developed using response surface methodology (RSM), and ideal parameters were determined; the reliability of the model was then tested.

Experimental method

A Furkan Kompakt 1 Z-NC model electrical discharge machine was used in the study. A test setup was designed and manufactured for use in graphite powder-mixed EDM experiments (Fig. 1). The setup consists of a dielectric tank, a circulation pump, two valves, and two sprayers. The dielectric tank is made of polypropylene for chemical corrosion resistance, and its side surfaces are angled to prevent graphite powder from settling on the tank bottom. The circulation pump circulates the dielectric fluid. One valve was installed at the lowest point of the system to drain the dielectric fluid in the tank after the machining was done. The other valve was located between the pump and the sprayers, and the dielectric flushing pressure was adjusted using this valve. One of the sprayers was used to maintain dielectric circulation within the tank. In contrast, the other was used to continuously supply the graphite powder-mixed dielectric fluid into the spark gap.

Kerosene was used as the dielectric fluid in the study, and 12.5 g/L graphite powder was mixed into the dielectric fluid in powder-mixed EDM experiments. The reasons for using graphite powder were that studies have shown that it increases conductivity, which has positive effects on machining speed and surface quality, and that it is well suspended in the dielectric fluid[11]. A nickel-based alloy called "remanium® CSE" was selected as the workpiece material (Fig. 2a, b). A copper electrode was used in the study due to copper's high electrical and thermal conductivity[26]. A chemical composition of nickel-based alloy is as shown in Table 1.

In the experiments, I, T_{on}, T_{off} and powder concentration were selected as variable parameters shown in Table 2. The machining depth was 2 mm, the open-circuit voltage was 130 V, the discharge voltage was 70 V, and the retraction distance was 2 mm; these settings were kept constant throughout the experiments. In all experiments, the workpiece was polarized positively and the electrode was polarized negatively. The I value used in the experiments were determined as 3, 6, and 12.5 A; the T_{on} values were 24, 48, and 99 µs; and the T_{off} values were 6, 12, and 24 µs. A total of 18 experiments were conducted.

Before and after each experiment, the workpiece and electrode used were weighed using a precision balance with a precision of 0.005 g, and MRR and EWR values were calculated by dividing the volumetric reduction by the machining time (Eqs. 1,2) and shown in Table 3. Further, the comparison of powder-mixed and non-powder-mixed EDM results is depicted in Table 4.

$$MRR = (change\ in\ volume\ of\ the\ workpiece)\ /\ (total\ machining\ time) \tag{1}$$

$$EWR = (change\ in\ volume\ of\ the\ electrode)\ /\ (total\ machining\ time) \tag{2}$$

After the experiment, the surface roughness of each workpiece was measured using the Mitutoyo Surftest SJ-310 surface roughness tester. The measuring standard was set to *I*SO 1997, profile = R, cutting values λc = 0.8 µm and λs = 2.5 µm, sampling length = 5 mm, traverse speed = 0.5 mm/s, and spacing = automatic.

Mathematical modelling

Response Surface Methodology (RSM) was used in mathematical modelling and optimization of the experimental results. The general formula of RSM for quadratic polynomials is given in Eq. 1.

$$Y = \beta_0 + \sum_{i=1}^{k} \beta_i X_i + \beta_i \sum_{i<j}^{k} \beta_{ij} X_i X_j + \sum_{i=1}^{k} \beta_{ii} X_i^2 \tag{3}$$

The β_0 term represents the initial state of all variables, the β_i term represents linear relationships, the β_{ii} term represents quadratic relationships, and the β_{ij} term represents binary relationships. The coefficients of the regression equation are then obtained by applying the least squares method[7].

Mathematical modelling of MRR

RSM analysis was performed for the graphite powder concentration, I, T_{on}, and T_{off} inputs, and the MRR output. The graphite powder concentration input was selected as categorical, while the other three inputs were selected as continuous. Variance analysis was then performed to determine the magnitude of the inputs' impact on the results. The F value in the variance analysis table indicates the effect of the parameter on the results. A larger F value indicates that the parameter has a greater impact on the outcome. The P value indicates the statistical significance of the parameter. Parameters with a P value of "zero" are the most significant parameters and must be included in the regression equation. Parameters with a P value greater than 0.05 have a low impact on the regression equation and can safely be eliminated from the equation[27]. The R-sq value represents the percentage

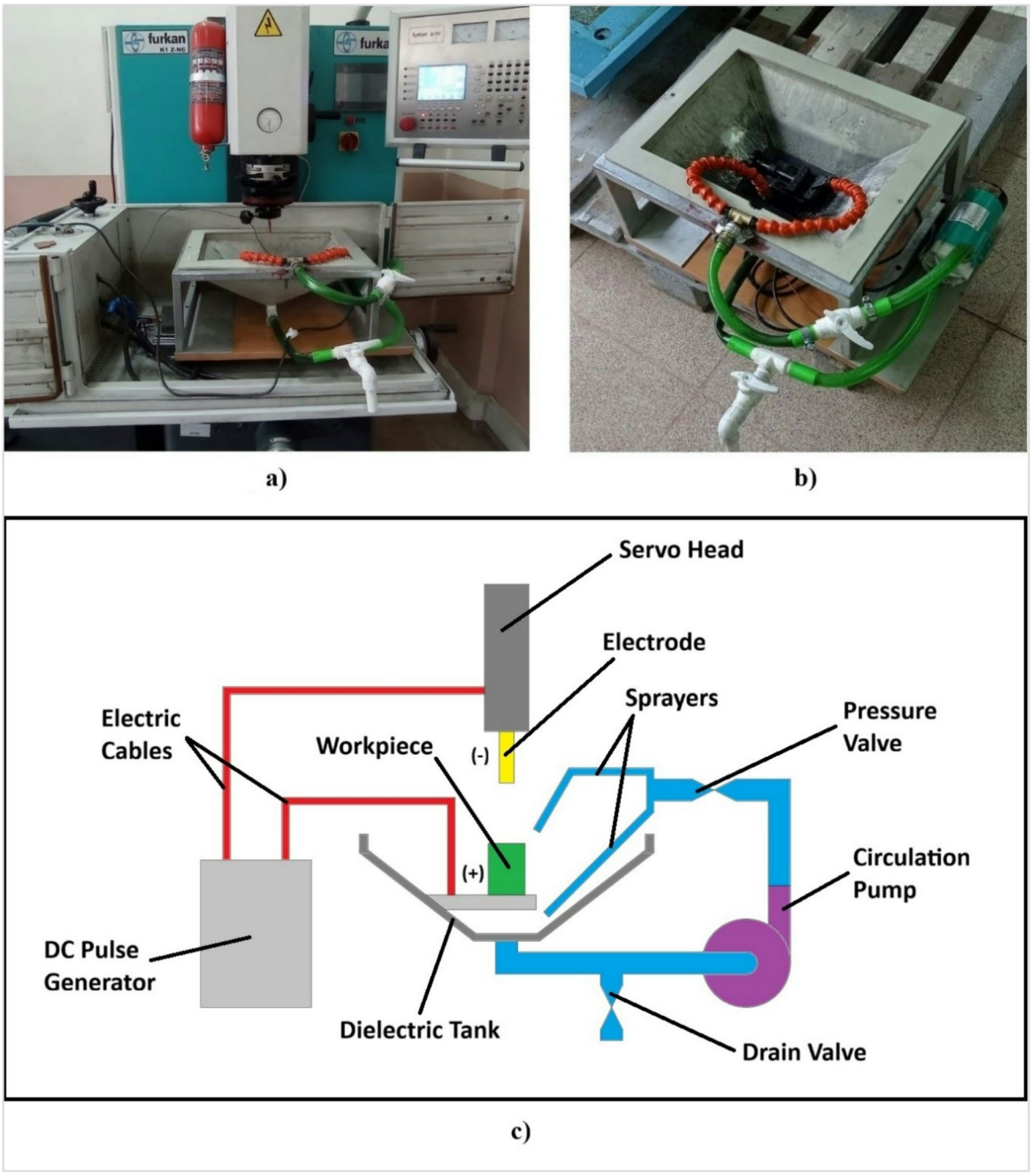

Fig. 1. Experimental equipment: (**a**) EDM machine, (**b**) experimental setup, (**c**) schematic of the machine setup.

of variation in the value calculated by the model. The R-sq(adj) value is the adjusted R-sq value, which is the percentage of variation in the results obtained by the model adjusted for the number of independent variables in the equation. R-sq(adj) is more effective than R-sq in indicating the reliability of regression equations with a large number of independent variables. R-sq and R-sq(adj) values close to 100% indicate high model reliability[28]. Table 5 shows the variance analysis results of the mathematical model created for MRR.

To increase the reliability of the model, terms with high P values were removed. The "T_{off}" term was not removed from the model despite its high P value because it is a direct experimental parameter. The results of the new analysis of variance are presented in Table 6.

Table 6 shows that the most influential parameters on MRR are I, T_{on}, $I^{*}T_{on}$ and graphite powder concentration, respectively. The T_{off} parameter has an insignificant effect on MRR. Two regression equations were created: one for the powder-mixed dielectric and the other for the dielectric without the powder additive. The equations are given in Eq. 2 and Eq. 3.

Fig. 2. (**a**) Workpiece before machining, (**b**) Workpiece after machining, (**c**) Copper electrodes used in experiments.

Element	Ni	Cr	Mo	Si	Fe
Chemical composition (% mass)	61	26	11	1,5	1,2

Table 1. Chemical composition of nickel-based alloy.

Machining conditions	Description
Dielectric fluid	Graphite powder-mixed kerosene
Electrode (Fig. 2c)	Copper electrode (8 mm diameter and 100 mm length, cylindrical shape)
Machining depth	2 mm
Open circuit voltage	130 V
Discharge voltage	70 V
Retraction distance	2 mm
Powder concentration	0; 12.5 g/L
Discharge current, *I*	3; 6; 12.5 A
Pulse-on time, T_{on}	24; 48; 99 µs
Pulse-off time, T_{off}	6; 12; 24 µs

Table 2. Machining parameters.

Experiment no.	Machining parameters				Results			
	Powder concentration (g/L)	I (A)	T_{on} (μs)	T_{off} (μs)	MRR (mm^3/min)	EWR (mm^3/min)		R_a (μm)
1	0	3	24	6	0.922	0.00545	3.234	
2	0	3	48	12	1.259	0.00768	3.312	
3	0	3	99	24	1.254	0.00726	3.882	
4	0	6	24	12	3.733	0.04380	5.265	
5	0	6	48	24	3.106	0.01947	6.952	
6	0	6	99	6	3.381	0.02049	6.013	
7	0	12.5	24	24	3.380	0.86097	5.829	
8	0	12.5	48	6	6.898	0.14766	6.829	
9	0	12.5	99	12	8.643	0.04098	8.931	
10	12.5	3	24	6	1.251	0.00962	3.294	
11	12.5	3	48	12	1.347	0.00963	3.696	
12	12.5	3	99	24	1.185	0.00798	3.599	
13	12.5	6	24	12	3.196	0.06051	4.736	
14	12.5	6	48	24	4.721	0.02842	5.699	
15	12.5	6	99	6	5.660	0.03431	4.795	
16	12.5	12.5	24	24	5.544	0.59260	4.251	
17	12.5	12.5	48	6	8.256	0.10350	6.778	
18	12.5	12.5	99	12	12.667	0.07627	7.047	

Table 3. Design of experiment and results.

	Mean results for experiments 1–9 (non-PM)		Mean results for experiments 10–18 (PM)	Percent change
MRR (mm3/min)	3.620		4.870	34.54%
EWR (mm3/min)	0.12820		0.10254	−20.01%
R_a (μm)	5.583		4.877	−12.64%

Table 4. Comparison of powder-mixed and non-powder-mixed EDM results.

Source	Degree of freedom	Adjusted sum of squares	Adjusted mean squares	F-value	*P*-value
Model	12	174.606	14.550	29.16	0.001
Linear	4	137.739	34.435	69.02	0
I	1	122.305	122.305	245.14	0
T_{on}	1	8.789	8.789	17.62	0.009
T_{off}	1	0.178	0.178	0.36	0.576
Dielectric	1	9.265	9.265	18.57	0.008
Square	3	2.209	0.736	1.48	0.328
I^2	1	2.176	2.176	4.36	0.091
T_{on}^2	1	0.016	0.016	0.03	0.865
T_{off}^2	1	0.019	0.019	0.04	0.853
2-Way interaction	5	15.773	3.155	6.32	0.032
I*T_{on}	1	9.238	9.238	18.52	0.008
I*T_{off}	1	1.269	1.269	2.54	0.172
I*Dielectric	1	4.301	4.301	8.62	0.032
T_{on}*Dielectric	1	1.638	1.638	3.28	0.130
T_{off}*Dielectric	1	0.003	0.003	0.01	0.940
Error	5	2.495	0.499		
Total	17	177.1			

Table 5. ANOVA results of the mathematical model created for MRR.

Source	Degree of freedom	Adjusted sum of squares	Adjusted mean squares	F-value	*P*-value
Model	6	168.619	28.103	36.45	0
Linear	4	160.853	40.213	52.15	0
I	1	130.206	130.206	168.87	0
T_{on}	1	22.328	22.328	28.96	0
T_{off}	1	0.07	0.07	0.09	0.769
Dielectric	1	8.561	8.561	11.1	0.007
2-Way interaction	2	17.875	8.937	11.59	0.002
*I**T_{on}	1	13.574	13.574	17.6	0.001
*I**Dielectric	1	4.301	4.301	5.58	0.038
Error	11	8.482	0.771		
Total	17	177.1			
R-sq = 95.21% and R-sq(adj) = 92.60%					

Table 6. ANOVA results of the adjusted mathematical model created for MRR.

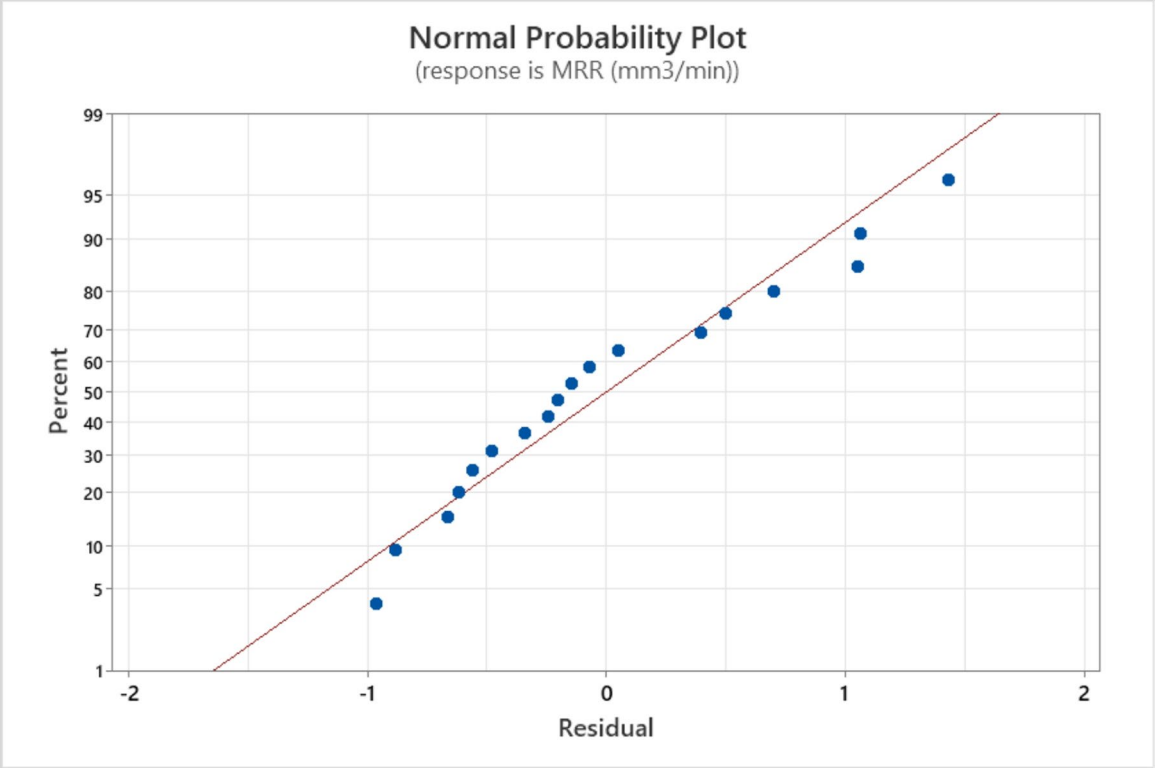

Fig. 3. Normal probability plot for MRR.

$$PM\ MRR\ (mm^3/min) = 1.015 + 0.307\ I - 0.0273\ T_{on} - 0.0098\ T_{off} + 0.00819\ I \times\ T_{on} \quad (4)$$

$$Non - PM\ MRR\ (mm^3/min) = 1.532 + 0.061\ I - 0.0273\ T_{on} - 0.0098\ T_{off} + 0.00819\ I \times\ T_{on} \quad (5)$$

Figure 3 shows the normal probability plot of the model created for MRR. In this plot, the red line represents the regression equation, the blue dots represent the experimental results, and the graph demonstrates the equation's compatibility with the experimental results. The horizontal axis represents the difference between the model's calculated value and the experimental data, and the vertical axis represents the percentage distribution.

Mathematical modelling of EWR

Then, RSM analysis was performed for EWR using the same inputs selected for MRR. The performance outputs and variance analysis results of the generated model are given in Table 7.

To increase the reliability of the model, values with high P values were removed. The results of the new analysis of variance are presented in Table 8.

Source	Degree of freedom	Adjusted sum of squares	Adjusted mean squares	F-value	*P*-value
Model	12	0887699	0.073975	26.52	0.001
Linear	4	0.323038	0.080760	28.95	0.001
I	1	0.248695	0.248695	89.16	0
T_{on}	1	0.017389	0.017389	6.23	0.055
T_{off}	1	0.041306	0.041306	14.81	0.012
Dielectric	1	0.004237	0.004237	1.52	0.273
Square	3	0.019525	0.006508	2.33	0.191
I^2	1	0.017089	0.017089	6.13	0.056
T_{on}^2	1	0.000973	0.000973	0.35	0.580
T_{off}^2	1	0.001372	0.001372	0.49	0.514
2-Way interaction	5	0.197684	0.039537	14.17	0.006
I*T_{on}	1	0.087164	0.087164	31.25	0.003
I*T_{off}	1	0.110369	0.110369	39.57	0.001
I*Dielectric	1	0.008524	0.008524	3.06	0.141
T_{on}*Dielectric	1	0.006333	0.006333	2.27	0.192
T_{off}*Dielectric	1	0.006129	0.006129	2.20	0.198
Error	5	0.013946	0.002789		
Total	17	0.901645			

Table 7. ANOVA results of the mathematical model created for EWR.

Source	Degree of freedom	Adjusted sum of squares	Adjusted mean squares	F-value	*P*-value
Model	6	0.847189	0.141198	28.52	0
Linear	4	0.370657	0.092664	18.72	0
I	1	0.300309	0.300309	60.66	0
T_{on}	1	0.017195	0.017195	3.47	0.089
T_{off}	1	0.045603	0.045603	9.21	0.011
Dielectric	1	0.002962	0.002962	0.6	0.455
2-Way interaction	2	0.269451	0.134726	27.21	0
I*T_{on}	1	0.112103	0.112103	22.64	0.001
I*T_{off}	1	0.178579	0.178579	36.07	0
Error	11	0.054457	0.004951		
Total	17	0.901645			
R-sq = 93.96% and R-sq(adj) = 90.67%					

Table 8. ANOVA results of the adjusted mathematical model created for EWR.

Table 8 shows that the most effective parameters on EWR are *I*, I*T_{off}, I*T_{on} and T_{off}, respectively. The effects of T_{on} and powder concentration on EWR are insignificant. Two regression equations were created: one for the dielectric with powder additive and the other for the dielectric without powder additive. The equations are given in Eq. 4 and Eq. 5.

$$PM\ EWR\ (mm^3/min) = -0.0794 + 0.0202\ I + 0.00462\ T_{on} - 0.02261\ T_{off} - 0.000747\ I \times\ T_{on} + 0.003938\ I \times\ T_{off} \quad (6)$$

$$Non - PM\ EWR\ (mm^3/min) = -0.0538 + 0.0202\ I + 0.00462\ T_{on} - 0.02261\ T_{off} -\ 0.000747\ I \times\ T_{on} + 0.003938\ I \times\ T_{off} \quad (7)$$

Figure 4 shows the normal probability graph of the model created for EWR.

Mathematical modelling of R_a

Finally, RSM analysis was performed for Ra using the same inputs selected for MRR. The performance outputs and variance analysis results of the generated model are given in Table 9.

To increase the reliability of the model, values with high P values were removed. The results of the new variance analysis are given in Table 10.

As seen in Table 10, the most influential parameter on R_a is *I*, followed by I^2, I*T_{on}, powder concentration, I*T_{off} and T_{on}. The effect of T_{off} on R_a is insignificant. Two regression equations were created: one for the dielectric with powder additive and the other for the dielectric without powder additive. The equations are given in Eq. 6 and Eq. 7.

$$PM\ R_a\ (\mu\, m) = 0{,}048 + 1.086\ I - 0.02508\ T_{on} + 0.1364\ T_{off} - 0.0548\ I^2 + 0.00446\ I \times\ T_{on} - 0.01577\ I \times\ T_{off} \quad (8)$$

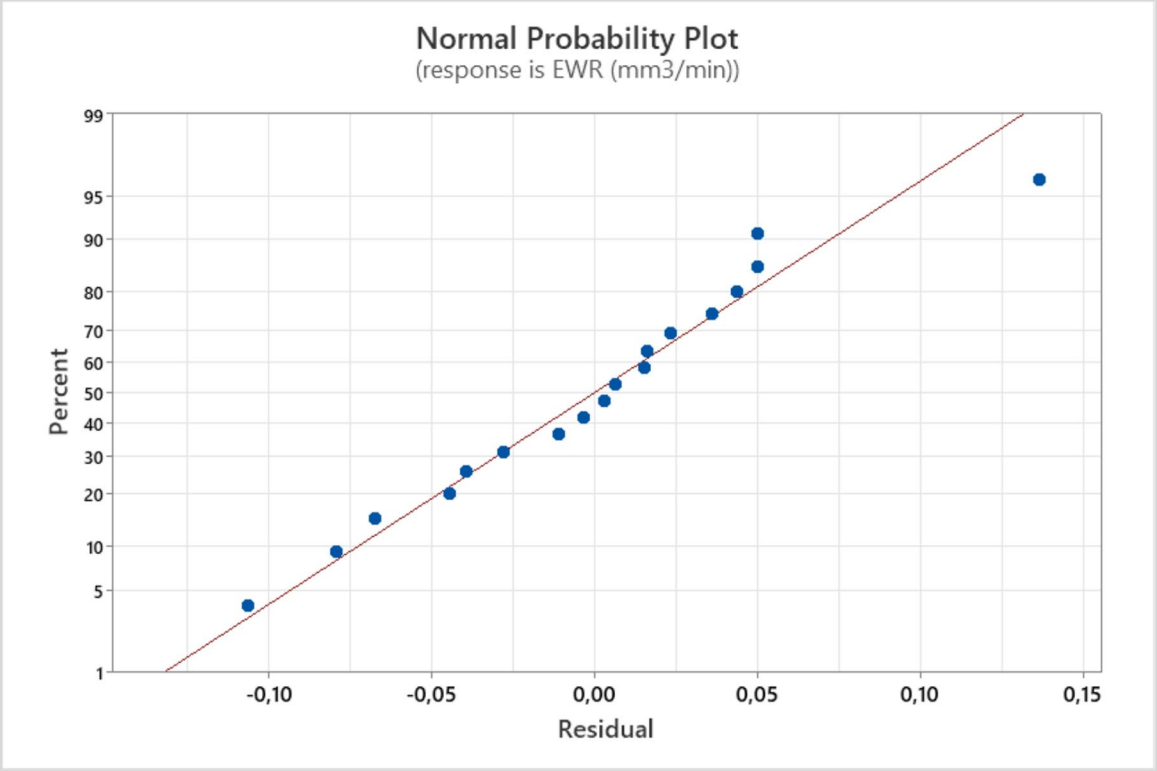

Fig. 4. Normal probability plot for EWR.

Source	Degree of freedom	Adjusted sum of squares	Adjusted mean squares	F-value	*P*-value
Model	12	46.635	3.886	25.59	0.001
Linear	4	34.305	8.576	56.47	0
I	1	30.550	30.550	201.17	0
T_{on}	1	1.669	1.669	10.99	0.021
T_{off}	1	0.256	0.256	1.68	0.251
Dielectric	1	3.371	3.371	22.19	0.005
Square	3	5.148	1.716	11.30	0.012
I^2	1	4.307	4.370	28.78	0.003
T_{on}^2	1	0.442	0.442	2.91	0.149
T_{off}^2	1	0.307	0.307	2.02	0.215
2-Way interaction	5	5.990	1.198	7.89	0.020
I*T_{on}	1	3.720	3.720	24.50	0.004
I*T_{off}	1	1.092	1.092	7.19	0.044
I*Dielectric	1	1.187	1.187	7.81	0.038
T_{on}*Dielectric	1	0.220	0.220	1.45	0.282
T_{off}*Dielectric	1	0.188	0.188	1.24	0.316
Error	5	0.759	0.152		
Total	17	47.394			

Table 9. ANOVA results of the mathematical model created for R_a.

$$Non-PM\ R_a\ (\mu m) = -0{,}124 + 1.216\,I - 0.02508\,T_{on} + 0.1364\ T_{off} - 0.0548\,I^2 + 0.00446\,I \times\ T_{on} - 0.01577\,I \times T_{off} \quad (9)$$

The normal probability graph of the model created for R_a is given in Fig. 5.

Discussion of experimental results

Main effects plots were created to determine the linear effects of machining parameters on the results. Figure 6 shows that MRR increases as I and T_{on} increase, while MRR decreases as T_{off} increases. As I increases, the

Source	Degree of freedom	Adjusted sum of squares	Adjusted mean squares	F-value	*P*-value
Model	8	45.4491	5.6811	26.29	0
Linear	4	33.221	8.3053	38.43	0
I	1	29.8038	29.8038	137.89	0
T_{on}	1	1.1447	1.1447	5.3	0.047
T_{off}	1	0.1469	0.1469	0.68	0.431
Dielectric	1	3.0487	3.0487	14.11	0.005
Square	1	4.3703	4.3703	20.22	0.001
I^2	1	4.3703	4.3703	20.22	0.001
2-way interaction	3	7.5402	2.5134	11.63	0.002
I*T_{on}	1	3.999	3.999	18.5	0.002
I*T_{off}	1	2.8629	2.8629	13.25	0.005
I*Dielectric	1	1.1866	1.1866	5.49	0.044
Error	9	1.9452	0.2161		
Total	17	47.3943			
R-sq = 95.90% and R-sq(adj) = 92.25%					

Table 10. ANOVA results of the adjusted mathematical model created for Ra.

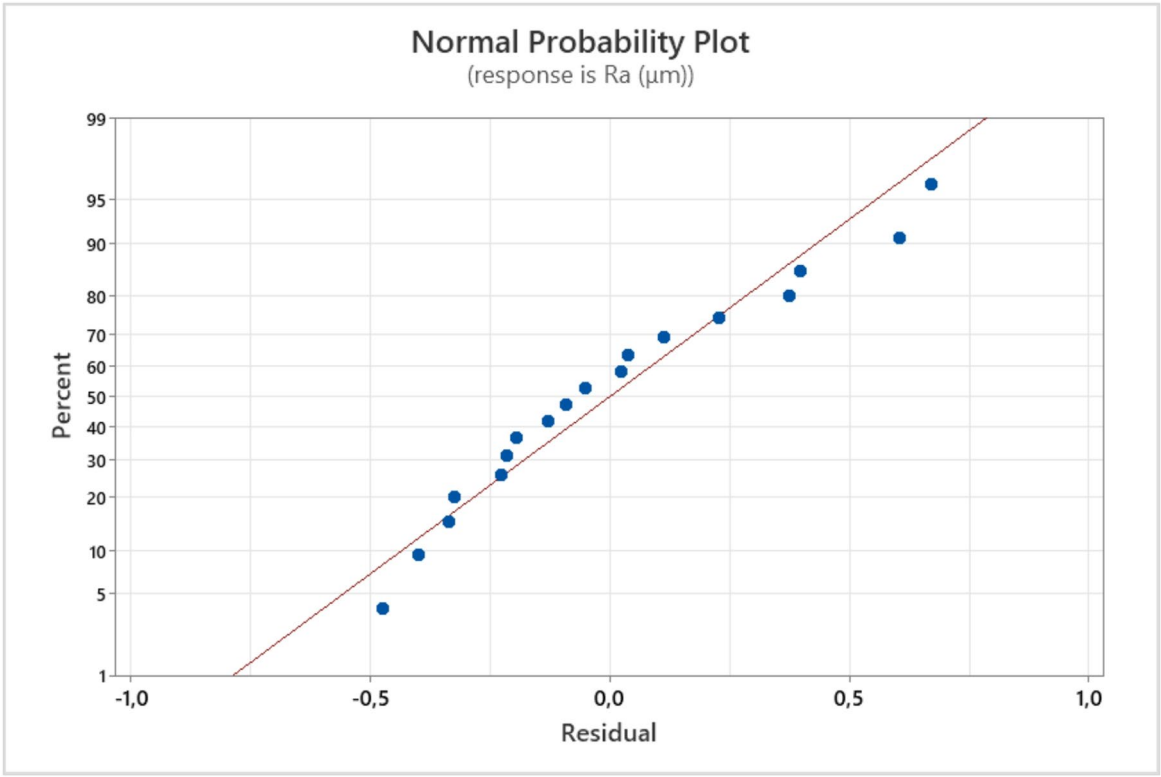

Fig. 5. Normal probability plot for R_a.

discharge energy increases, and as T_{on} increases, discharges last longer. These two factors cause each discharge to remove a larger volume of material from the workpiece. No machining occurs during T_{off}[29]. The results are consistent with theoretical data. The use of powder-mixed dielectric has been shown to increase MRR. The use of a powder-mixed dielectric has a positive effect on MRR by facilitating electrical discharge and shortening spark delay.

Figure 7 shows that EWR decreases as T_{on} increases and it increases as I, T_{off} increase. As I increases, discharge energy increases, which results in greater material erosion from the electrode as well as the workpiece. When T_{on} is kept short, heat does not spread throughout the electrode but remains only in the spark zone. However, when T_{on} is increased, thanks to copper's good thermal conductivity, heat spreads throughout the electrode, reducing the heat accumulated on the surface in contact with the workpiece. Furthermore, because more material erosion occurs with a single discharge at longer T_{on} values, the total number of discharges during machining is reduced[29].

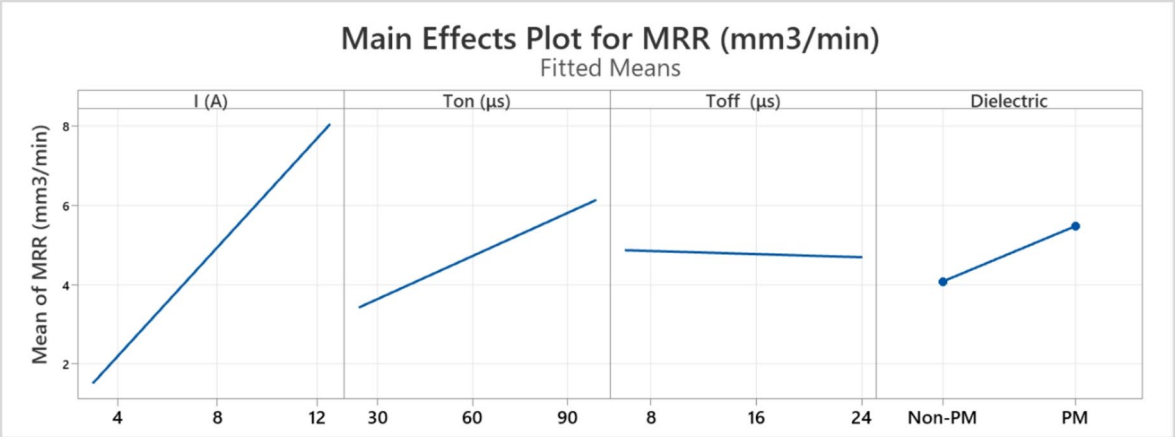

Fig. 6. Main effects plot for MRR.

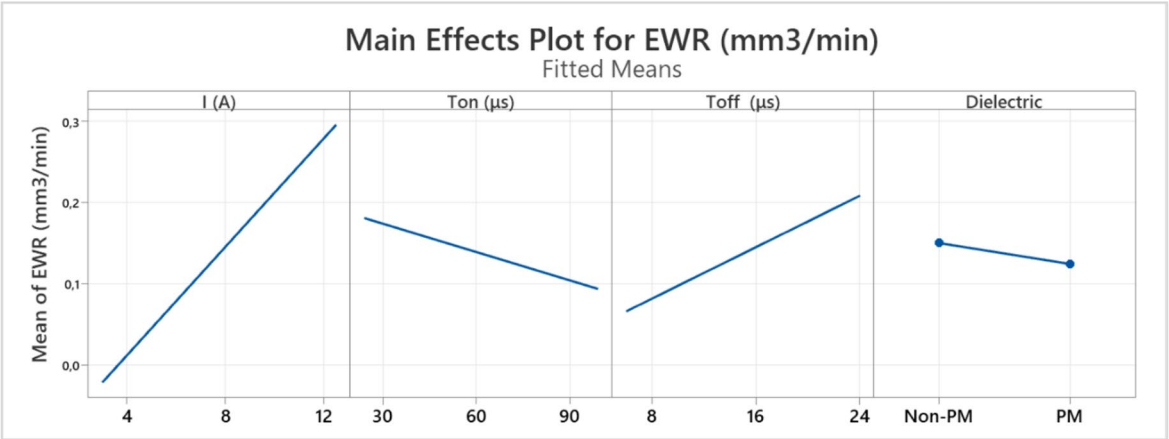

Fig. 7. Main effects plot for EWR.

It is thought that this is why the EWR decreases when *I* is decreased and T_{on} is increased. Lower EWR has been obtained with the powder-mixed dielectric but ANOVA results show that effect of using powder mixed dielectric was insignificant on this parameter.

Figure 8 shows that R_a first increases and then decreases as *I* increases and that it increases as T_{on} and T_{off} increase. Lower R_a values have been obtained by using powder mixed dielectric. This is more evident in machining experiments conducted with high *I*.

Optimization of parameters and verification experiment

Parameter optimization was performed after obtaining regression equations for all three performance outcomes. Minimum Ra, minimum EWR, and maximum MRR were determined as the ideal machining performance approach. Since none of the output parameters were prioritized over others, the weights and importances of all targets were taken as "one" (Table 11).

As seen in Fig. 9, the ideal processing parameters for the highest MRR, lowest EWR, and lowest R_a were found to be *I* = 12.5 A, T_{on}=66,4242µs, T_{off}=6µs, and a powder-mixed dielectric. With the selected parameters, the minimum Ra requirement was fulfilled by 38.498%, the minimum EWR requirement was fulfilled by 98.291%, and the maximum MRR requirement was fulfilled by 75.453%. The composite desirability was 65.85%. Due to the direct proportionality between MRR and Ra, low R_a and high MRR could not be achieved at the same time[29].

Because specific *I*, T_{on}, and T_{off} values can be selected on the EDM machine where the experiments were performed, the machining parameters for the verification experiment were rounded to the nearest available values. In the final case, the machining parameters were determined as *I* = 12.5 A, T_{on}=66 µs, T_{off}=6 µs, and powder-mixed dielectric. The developed model predicted an MRR of 9.75245 mm^3/min, an EWR of 0.0220672 mm^3/min, and an R_a of 6.72466 µm. The validation experiment yielded an MRR of 8.06939 mm^3/min, an EWR of 0.0188632 mm^3/min, and a R_a of 6.805 µm. Accordingly, the developed model predicted MRR with a deviation of −1.68306 mm^3/min and a 20.86% error, EWR with a deviation of −0.003204 mm^3/min and a 16.99% error, and R_a with a deviation of 0.08034 µm and a 1.18% error (Table 12).

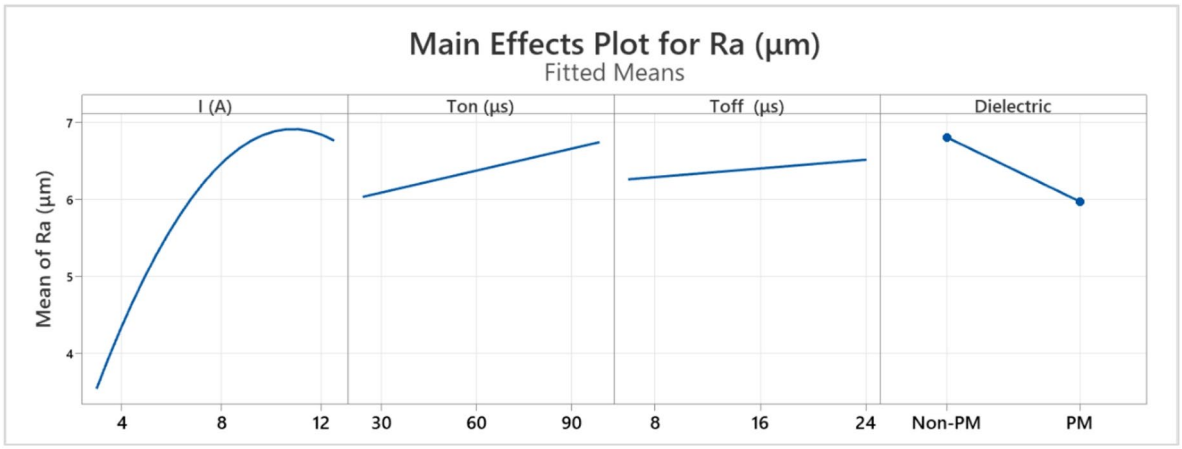

Fig. 8. Main effects plot for R_a.

Response	Goal	Lower limit	Target value	Upper limit	Weight	Importance
R_a (µm)	Minimum		3.2337	8.931	1	1
EWR (mm^3/min)	Minimum		0.0054	0.86097	1	1
MRR (mm^3/min)	Maximum	0.92237	12.6674		1	1

Table 11. Optimization parameters.

Conclusions

In this study, the optimum machining parameters for the nickel-based alloy "remanium® CSE" (which has not previously been investigated for machinability by EDM) to achieve high MRR, low EWR, and R_a were determined, and the effects of graphite powder addition were investigated. Experiments were conducted using a specially designed setup, using a copper electrode and a graphite powder-mixed dielectric fluid. Graphite powder concentration, current, T_{on}, and T_{off} were selected as variable parameters. The findings were evaluated using ANOVA, and a mathematical model was developed using RSM, and the model was validated by conducting validation experiments. The key numerical results and findings obtained from the study are as follows:

- The highest MRR was measured as 12.667 mm^3/min with I = 12.5 A, T_{on}=99µs, T_{off}=12µs and powder-mixed dielectric; the lowest MRR was measured as 0.922 mm^3/min with I = 3 A, T_{on}=24µs, T_{off}=6µs and non-powder-mixed dielectric.
- The most influential parameters on MRR are I, T_{on}, and powder concentration, respectively. The effect of T_{off} on MRR is insignificant. It has been found that MRR increases with I, T_{on} and decreases with T_{off}.
- The highest EWR was measured as 0.86097 mm^3/min with I = 12.5 A, T_{on}=24µs, T_{off}=24µs and non-powder-mixed dielectric; the lowest EWR was measured as 0.00545 mm3/min with I = 3 A, T_{on}=24µs, Toff = 6µs and non-powder-mixed dielectric.
- The most influential parameters on EWR are I and T_{off}. T_{on} and powder concentration have a insignificant effect on EWR. EWR has been found to increase as I and T_{off} increase, and to decrease as T_{on} increases.
- The lowest R_a was measured as 3.234 µm with I = 3 A, T_{on}=24µs, T_{off}=6µs non-powder-mixed dielectric; the highest R_a was measured as 8.931 µm with I = 12.5 A, T_{on}=99µs, T_{off}=12µs and non-powder-mixed dielectric.
- The most influential parameters on R_a are I, powder concentration, and T_{on}, respectively. The effect of T_{off} on R_a is insignificant.
- Better results were obtained in all performance outputs when powder mixed dielectric was used. On average, MRR increased by 34.54%, EWR decreased by 20.01% and R_a decreased by 12.64% on powder mixed EDM experiments compared to experiments done with same parameters but without powder additive in the dielectric.
- Parameter optimization was performed using the developed model with target outputs of the highest MRR, lowest EWR, and lowest R_a. The model determined the ideal machining parameters as I = 12.5 A, T_{on}=66µs, T_{off}=6µs, and a powder-mixed dielectric. According to the validation experiment, the model predicted MRR with a 20.86% error, EWR with a 16.99% error, and R_a with a 1.18% error.

Shaping this metal alloy using EDM provides a superior solution for dentistry, mould-making, and biomedical applications, ensuring high surface quality, minimal electrode wear, and precise machining of complex geometries. Furthermore, the addition of graphite powder significantly increases efficiency and lowers production costs by shortening machining times and reducing electrode wear.

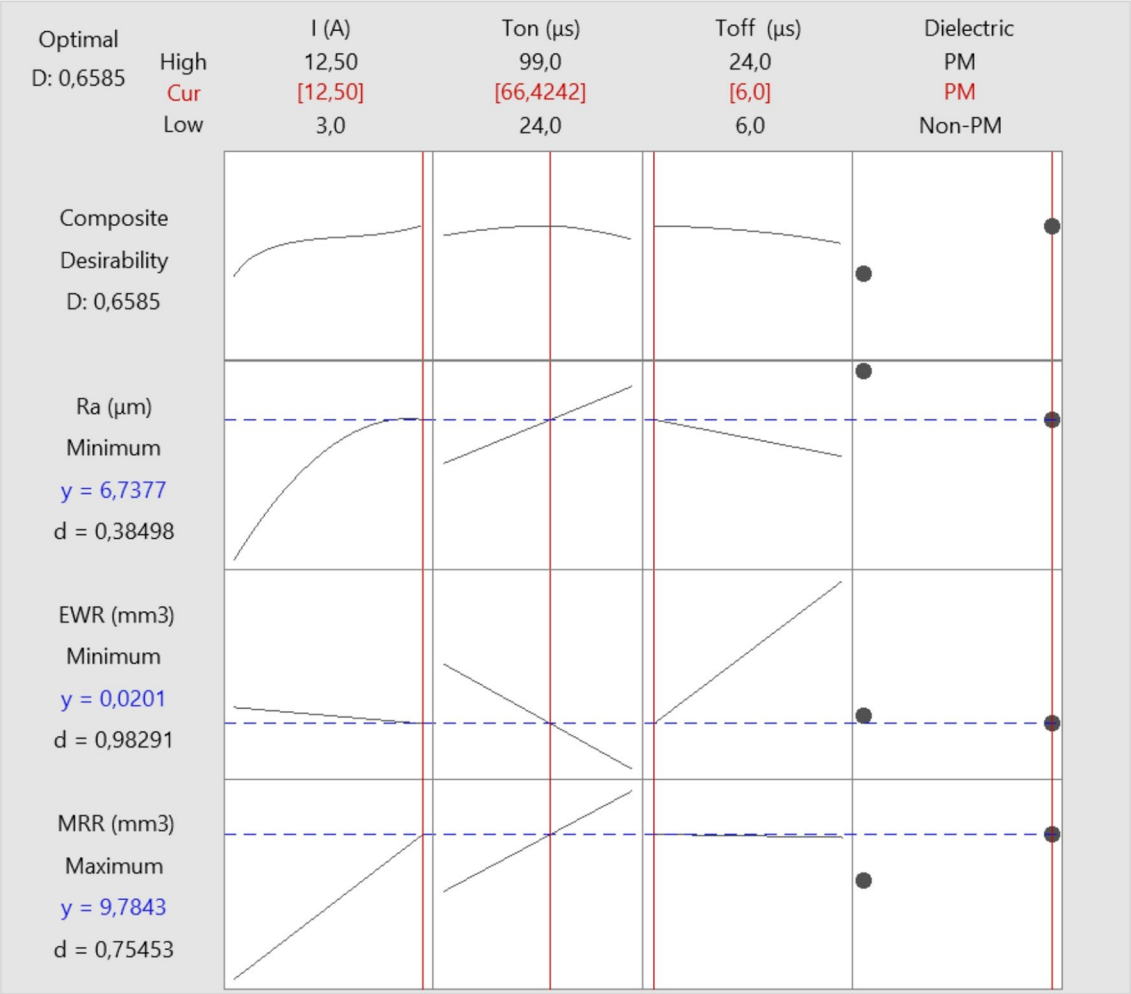

Fig. 9. Optimization results.

Response type	Experimental value	Predicted value	Deviation	Percent error (%)
MRR (mm^3/min)	8.06939	9.75245	−1.68306	20.86%
EWR (mm^3/min)	0.0188632	0.0220672	−0.003204	16.99%
R_a (µm)	6.805	6.72466	0.08034	1.18%

Table 12. Comparison of experimental results with predicted results.

Data availability

Data will be made available upon request. Contact the Corresponding Author if someone wants to request the data from this study.

Received: 10 October 2025; Accepted: 8 December 2025
Published online: 18 December 2025

References

1. Jeswani, M. L. Effect of the addition of graphite powder to kerosene used as the dielectric fluid in electrical discharge machining. *Wear* **70** (2), 133–139. https://doi.org/10.1016/0043-1648(81)90148-4 (1981).
2. Kansal, H. K., Singh, S. & Kumar, P. Parametric optimization of powder mixed electrical discharge machining by response surface methodology. *J. Mater. Process. Technol.* **169** (3), 427–436. https://doi.org/10.1016/j.jmatprotec.2005.03.028 (2005).
3. Kung, K. Y., Horng, J. T. & Chiang, K. T. Material removal rate and electrode wear ratio study on the powder mixed electrical discharge machining of cobalt-bonded tungsten carbide. *Int. J. Adv. Manuf. Technol.* **40**, 1–2. https://doi.org/10.1007/s00170-007-1307-2 (2009).
4. Kumar, H. & Davim, J. P. Role of powder in the machining of Al-10%Sic_p metal matrix composites by powder mixed electric discharge machining. *J. Compos. Mater.* **45** (2), 133–151. https://doi.org/10.1177/0021998310371543 (2011).

5. Bhattacharya, A., Batish, A., Singh, G. & Singla, V. K. Optimal parameter settings for rough and finish machining of die steels in powder-mixed EDM. *Int. J. Adv. Manuf. Technol.* **61**, 5–8. https://doi.org/10.1007/s00170-011-3716-5 (2012).
6. Singh, S. & Yeh, M. F. Optimization of abrasive powder mixed EDM of aluminum matrix composites with multiple responses using Gray relational analysis. *J. Mater. Eng. Perform.* **21** (4), 481–491. https://doi.org/10.1007/s11665-011-9861-z (2012).
7. Assarzadeh, S. & Ghoreishi, M. A dual response surface-desirability approach to process modeling and optimization of Al2O3 powder-mixed electrical discharge machining (PMEDM) parameters. *Int. J. Adv. Manuf. Technol.* **64**, 9–12. https://doi.org/10.1007/s00170-012-4115-2 (2013).
8. Jabbaripour, B., Sadeghi, M. H., Shabgard, M. R. & Faraji, H. Investigating surface roughness, material removal rate and corrosion resistance in PMEDM of γ-TiAl intermetallic. *J. Manuf. Process.* **15** (1), 56–68. https://doi.org/10.1016/j.jmapro.2012.09.016 (2013).
9. Singh, A. K., Kumar, S. & Singh, V. P. Effect of the addition of conductive powder in dielectric on the surface properties of superalloy super Co 605 by EDM process. *Int. J. Adv. Manuf. Technol.* **77**, 1–4. https://doi.org/10.1007/s00170-014-6433-z (2015).
10. Talla, G., Sahoo, D. K., Gangopadhyay, S. & Biswas, C. K. Modeling and multi-objective optimization of powder mixed electric discharge machining process of aluminum/alumina metal matrix composite. *Eng. Sci. Technol. Int. J.* **18** (3), 369–373. https://doi.org/10.1016/j.jestch.2015.01.007 (2015).
11. Unses, E. & Cogun, C. Improvement of electric discharge machining (EDM) performance of Ti-6Al-4V alloy with added graphite powder to dielectric. *Stroj Vestn – J. Mech. Eng.* **61** (6), 409–418. https://doi.org/10.5545/sv-jme.2015.2460 (2015).
12. Long, B. T., Phan, N. H., Cuong, N. & Jatti, V. S. Optimization of PMEDM process parameter for maximizing material removal rate by taguchi's method. *Int. J. Adv. Manuf. Technol.* **87**, 5–8. https://doi.org/10.1007/s00170-016-8586-4 (2016).
13. Tripathy, S. & Tripathy, D. K. Multi-attribute optimization of machining process parameters in powder mixed electro-discharge machining using TOPSIS and grey relational analysis. *Eng. Sci. Technol. Int. J.* **19** (1), 62–70. https://doi.org/10.1016/j.jestch.2015.07.010 (2016).
14. Mohal, S. & Kumar, H. Parametric optimization of multiwalled carbon nanotube-assisted electric discharge machining of Al-10%SiC_p metal matrix composite by response surface methodology. *Mater. Manuf. Process.* **32** (3), 263–273. https://doi.org/10.1080/10426914.2016.1140196 (2017).
15. Banh, T. L., Nguyen, H. P., Ngo, C. & Nguyen, D. T. Characteristics optimization of powder mixed electric discharge machining using titanium powder for die steel materials. *Proc. Inst. Mech. Eng. Part E J. Process Mech. Eng.* **232**(3), 281–298. https://doi.org/10.1177/0954408917693661 (2018).
16. Mohanty, S., Mishra, A., Nanda, B. K. & Routara, B. C. Multi-objective parametric optimization of nano powder mixed electrical discharge machining of AlSiCp using response surface methodology and particle swarm optimization. *Alex Eng. J.* **57** (2), 609–619. https://doi.org/10.1016/j.aej.2017.02.006 (2018).
17. Jadam, T., Sahu, S. K., Datta, S. & Masanta, M. EDM performance of inconel 718 superalloy: application of multi-walled carbon nanotube (MWCNT) added dielectric media. *J. Braz Soc. Mech. Sci. Eng.* **41** (8), 305. https://doi.org/10.1007/s40430-019-1813-9 (2019).
18. Sahu, S. K. & Datta, S. Experimental studies on graphite powder-mixed electro-discharge machining of Inconel 718 super alloys: Comparison with conventional electro-discharge machining. *Proc. Inst. Mech. Eng. Part E J. Process Mech. Eng.* **233**(2), 384–402. https://doi.org/10.1177/0954408918787104 (2019).
19. Alhodaib, A., Shandilya, P., Rouniyar, A. K. & Bisaria, H. Experimental investigation on silicon powder Mixed-EDM of Nimonic-90 Superalloy. *Metals* **11** (11), 1673. https://doi.org/10.3390/met11111673 (2021).
20. Ramesh, S. & Jenarthanan, M. Optimizing the powder mixed EDM process of nickel based super alloyOptimizing the powder mixed EDM process of nickel based super alloy. *Proc. Inst. Mech. Eng. Part E J. Process Mech. Eng.* **235**(4), 1092–1103. https://doi.org/10.1177/09544089211002782 (2021).
21. Chakraborty, S., Mitra, S. & Bose, D. An investigation on dimensional accuracy and surface topography in powder mixed WEDM using RSM and GRA-PCA. *Mater. Today Proc.* **44**, 1524–1530. https://doi.org/10.1016/j.matpr.2020.11.734 (2021).
22. Chakraborty, S., Mitra, S. & Bose, D. Evaluation of response characteristics using sensitivity analysis and TLBO technique of powder mixed wire EDM of Ti6Al4V alloy. *CIRP J. Manuf. Sci. Technol.* **47**, 260–272. https://doi.org/10.1016/j.cirpj.2023.11.004 (2023).
23. Le, V. T. et al. Optimization and comparison of machining characteristics of SKD61 steel in powder-mixed EDM process by TOPSIS and desirability approach. *Int. J. Adv. Manuf. Technol.* **130**, 1–2. https://doi.org/10.1007/s00170-023-12680-8 (2024).
24. Le, V. T., Nguyen, T. H. M. & Hoang, T. D. Machining characteristics of different tool electrodes during PMEDM for machining X40CrMoV51 alloy: an investigative and comparative study. *Ceram. Int.* https://doi.org/10.1016/j.ceramint.2025.10.347 (2025).
25. Ho, K. H. & Newman, S. T. State of the Art electrical discharge machining (EDM). *Int. J. Mach. Tools Manuf.* **43** (13), 1287–1300. https://doi.org/10.1016/S0890-6955(03)00162-7 (2003).
26. Işık, A. T. Semente Karbürün Elektro Erozyon ile İşlenmesinde İşleme Parametrelerinin Optimizasyonu, Doctoral Dissertion, Karabük University Graduate School of Natural and Applied Sciences, Karabük, (2022).
27. Kul, S. Interpretation of statistical results: what is p value and confidence interval? *Plevra Bul.* **8** (1), 11–13. https://doi.org/10.5152/pb.2014.003 (2014).
28. Ayhan, E. Elektrokimyasal delme işleminde delik kalitesinin iyileştirilmesi üzerine bir çalışma, Doctoral Dissertion, Gazi University Graduate School of Natural and Applied Sciences, Ankara, (2023).
29. El-Hofy, H. *Fundamentals of machining processes: conventional and nonconventional processes*, Third edition. Boca Raton London: CRC Press/Taylor & Francis Group, (2019).

Author contributions

Concept: Emin Salih San, Hacı Bekir Özerkan, Mehmet SubaşıDesign: Emin Salih San, Robert ČepLiterature: Emin Salih San, Hacı Bekir Özerkan, Mehmet Subaşı, Emre Ayhan, Sachin Salunkhe, Emad S. Abouel Nasr, Robert ČepMethodology: Emre Ayhan, Sachin Salunkhe, Emad S. Abouel Nasr, Robert ČepTesting: Emin Salih San, Hacı Bekir Özerkan, Mehmet Subaşı, Emre Ayhan, Ahmet Mave, Sachin Salunkhe, Emad S. Abouel Nasr, Robert ČepReview: Emin Salih San, Hacı Bekir Özerkan, Mehmet Subaşı, Emre Ayhan, Ahmet Mave, Sachin Salunkhe, Emad S. Abouel Nasr, Robert ČepEditing: Emin Salih San, Hacı Bekir Özerkan, Mehmet Subaşı, Emre Ayhan, Ahmet Mave, Sachin Salunkhe, Emad S. Abouel Nasr, Robert ČepFunding: Emad S. Abouel Nasr, Robert Čep.

Funding

The authors also extend their appreciation to King Saud University for funding the publication of this work through Researchers Supporting Project number (ORF2025R164), King Saud University, Riyadh, Saudi Arabia. This article was co-funded by the European Union under the REFRESH – Research Excellence for Region Sustainability and High-tech Industries project number CZ.10.03.01/00/22_003/0000048 via the Operational Programme Just Transition and has been done in connection with project Students Grant Competition SP2024/087 "Specific Research of Sustainable Manufacturing Technologies" financed by the Ministry of Education, Youth

and Sports and Faculty of Mechanical Engineering VŠB-TUO. Article has been done in connection with project Students Grant Competition SP2024/087 "Specific Research of Sustainable Manufacturing Technologies" financed by the Ministry of Education, Youth and Sports and Faculty of Mechanical Engineering VŠB-TUO.

Declarations

Competing interests

The authors declare no competing interests.

Additional information

Correspondence and requests for materials should be addressed to H.B.Ö. or S.S.

Reprints and permissions information is available at www.nature.com/reprints.

Publisher's note Springer Nature remains neutral with regard to jurisdictional claims in published maps and institutional affiliations.